© 2014. Published by The Company of Biologists Ltd | Development (2014) 141, 2866-2874 doi:10.1242/dev.105932

RESEARCH ARTICLE

# Prickle/spiny-legs isoforms control the polarity of the apical microtubule network in planar cell polarity

**Jessica Olofsson[1,*], Katherine A. Sharp[1,2,*], Maja Matis[1], Bomsoo Cho[1] and Jeffrey D. Axelrod[1,‡]**


## ABSTRACT

Microtubules (MTs) are substrates upon which plus- and minus-end directed motors control the directional movement of cargos that are essential for generating cell polarity. Although centrosomal MTs are organized with plus-ends away from the MT organizing center, the regulation of non-centrosomal MT polarity is poorly understood. Increasing evidence supports the model that directional information for planar polarization is derived from the alignment of a parallel apical network of MTs and the directional MT-dependent trafficking of downstream signaling components. The Fat/Dachsous/Four-jointed (Ft/Ds/Fj) signaling system contributes to orienting those MTs. In addition to previously defined functions in promoting asymmetric subcellular localization of 'core' planar cell polarity (PCP) proteins, we find that alternative Prickle (Pk-Sple) protein isoforms control the polarity of this MT network. This function allows the isoforms of Pk-Sple to differentially determine the direction in which asymmetry is established and therefore, ultimately, the direction of tissue polarity. Oppositely oriented signals that are encoded by oppositely oriented Fj and Ds gradients produce the same polarity outcome in different tissues or compartments, and the tissue-specific activity of alternative Pk-Sple protein isoforms has been observed to rectify the interpretation of opposite upstream directional signals. The control of MT polarity, and thus the directionality of apical vesicle traffic, by Pk-Sple provides a mechanism for this rectification.


**KEY WORDS: Prickle, Spiny-legs, Microtubules, Planar cell polarity, Vesicle transport, *Drosophila***

## INTRODUCTION

Microtubule (MT)-based vesicle transport is a fundamental mechanism that controls the spatial organization of nearly all animal cells. The directed trafficking of cargos allows cells to differentiate one side of the cell from the other, to build and maintain specialized structures at specified locations, and to allow cells to grow in size or spread directionally (Müsch, 2004). These features are crucial both in development, such as during specification of different sides of epithelial sheets (apical-basal polarity), as well as for controlling physiological processes, such as the maintenance and regulation of activities at neuronal synaptic junctions. MTs are polarized, and much attention has been given to how vesicle transport can proceed towards the plus- or minus-ends of MTs. By contrast, less is known about how non-centrosomal MT arrays, on which trafficking occurs, are formed or how their polarity is regulated.

Planar cell polarity (PCP) is the polarity of epithelial cells orthogonal to their apical-basal axis. Several molecular modules regulate PCP in *Drosophila* (Axelrod, 2009). The core module coordinates polarity between neighboring cells and acts as an amplifier, producing asymmetric subcellular localization of core PCP proteins to proximal (or anterior) and distal (or posterior) apical junctions (Axelrod, 2009; Goodrich and Strutt, 2011). This localization is thought to mark cellular asymmetry for subsequent morphological polarization, such as the directional growth of trichomes (or hairs) on the adult cuticle. Coordination and amplification of polarity are mediated by Fmi (Stan – FlyBase) homodimer-dependent interactions between proximal [Van Gogh (Vang), Prickle (also known as Pk-Sple)] and distal [Frizzled (Fz), Dishevelled (Dsh)] proteins across intercellular boundaries (Casal et al., 2006; Strutt and Strutt, 2007, 2008; Chen et al., 2008; Wu and Mlodzik, 2008) and by mutual exclusion of oppositely oriented complexes (Tree et al., 2002; Amonlirdviman et al., 2005).

In the fly wing, the Fat/Dachsous/Four-jointed (Ft/Ds/Fj) module aligns an apical non-centrosomal MT network (Fristrom and Fristrom, 1975; Eaton et al., 1996; Turner and Adler, 1998; Harumoto et al., 2010). The graded expression of Fj and Ds produces a slight excess of Ft activity on the proximal and Ds activity on the distal side of each cell (Yang et al., 2002; Ma et al., 2003; Ambegaonkar et al., 2012; Bosveld et al., 2012; Brittle et al., 2012) (Fig. 1A). These proteins, either directly or indirectly, organize MTs into proximal-distal oriented tracks with a subtle excess of plus-ends on the distal side of the cell (Fig. 1B) (Shimada et al., 2006; Harumoto et al., 2010). Plus-end directed transport of vesicles containing Fz biases the movement of Fz towards the distal side of the cell, which is likely to influence the direction of core module polarization (Shimada et al., 2006; Harumoto et al., 2010). However, the relationship between the direction of the Fj and Ds gradients and the direction of core module polarization is not conserved in all tissues. In wing and posterior abdomen (P-abd), Dsh and Fz accumulate towards areas of high Fj and low Ds expression, whereas in eye and anterior abdomen (A-abd), they accumulate towards areas of low Fj and high Ds expression (Zeidler et al., 2000; Casal et al., 2002; Ma et al., 2003; Matakatsu and Blair, 2004; Rogulja et al., 2008; Axelrod, 2009), thus presenting a signal rectification paradox and perhaps calling into question the validity of this model.

Although the formation of this parallel network of apical MTs is dependent on the 'Ft/Ds/Fj' module (Harumoto et al., 2010), here we show that the bias in the direction of MT plus-ends within the network is dependent upon alternative Pk-Sple protein isoforms, Prickle$^{pk}$ (Pk) and Prickle$^{spiny\text{-}legs}$ (Sple), which are the products of alternative splicing that encode different N-termini (supplementary material Fig. S2A). We propose that the function of these isoforms is distinct from that of Pk-Sple in amplifying the asymmetric localization of core module components (Strutt and Strutt, 2009). The ability of Pk and Sple to bias the polarity of the apical MT

[1]Department of Pathology, Stanford University School of Medicine, 300 Pasteur Drive, L235, Stanford, CA 94305, USA. [2]Department of Genetics, Stanford University School of Medicine, 300 Pasteur Drive, L235, Stanford, CA 94305, USA.
*These authors contributed equally to this work

‡Author for correspondence (jaxelrod@stanford.edu)

**Received 11 November 2013; Accepted 19 May 2014**

Development (2014) 141, 2866-2874 doi:10.1242/dev.105932

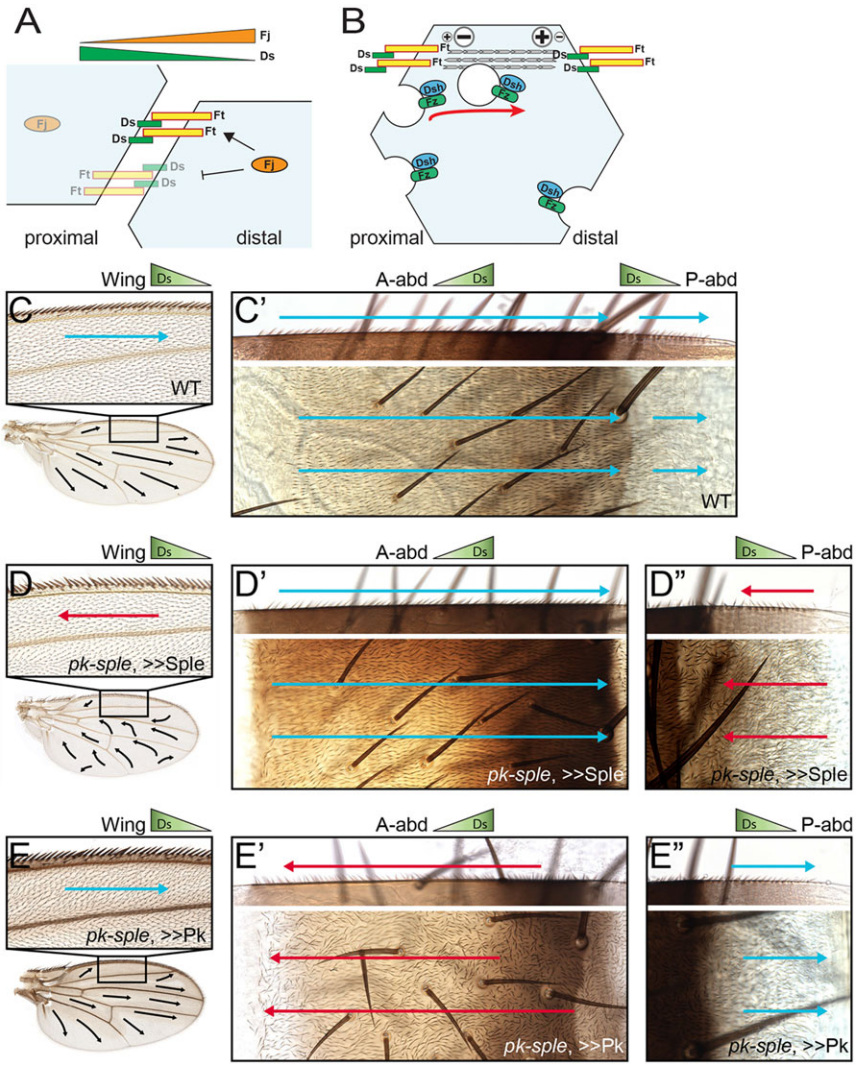


**Fig. 1. Pk and Sple produce opposite directions of hair growth.** (A) Graded expression of Fj and Ds results in asymmetrically distributed Ft/Ds heterodimers. Faded symbols represent species at reduced concentration relative to bright ones. (B) In the wing, Ft/Ds heterodimers organize MTs (gray) that serve as substrates for the directed trafficking of vesicles containing Dsh and/or Fz. There is a bias of MT plus-ends at the distal side of the cell, and polarized delivery of Dsh towards MT plus-ends thus provides input bias in order to orient core PCP module polarization. Red arrow indicates directional bias of transport. (C-E″) Direction of hair growth in wing and abdomen in wild type (wt) (C,C′) and in flies in which endogenous Pk and Sple have been removed and Sple (D-D″) or Pk (E-E″) reconstituted (>>Sple and >>Pk, respectively) through *D174Gal4*-driven expression (wing), *ciGal4*-driven expression (A-abd) or *hhGal4*-driven expression (P-abd). See supplementary material Fig. S3 for the expression pattern of *D174Gal4*. Blue arrows indicate normal hair direction; red arrows indicate a reversed hair polarity. Green slopes illustrate the direction of the Ds gradient in each tissue. The penetrance of the phenotypes in C-E″ was virtually complete.

network in opposite orientations relative to the gradients of the Ft/Ds/Fj module provides a mechanism for the rectification of these opposite upstream signals across various tissues.

## RESULTS

### Pk-Sple isoform expression determines the direction of hair growth

PCP in various fly tissues depends on either the Pk or the Sple isoform of Pk-Sple. For example, *sple* wings have normal hair polarity whereas *pk* wings have severely disrupted hair polarity (Gubb et al., 1999). These results suggest that one isoform is more highly expressed, or active, in each compartment. We confirmed this genetic evidence suggesting that Pk is the predominantly expressed isoform in wild-type wings by using western blot. Pk was the predominant isoform from third instar to 28 h after pupal formation (APF), whereas small amounts of Sple were detectable in third instar and the levels decreased further in early pupal wing (Fig. 2A). Overexpressing Sple in wings produces varying degrees of polarity reversal (supplementary material Fig. S1) (Gubb et al., 1999; Lee and Adler, 2002; Doyle et al., 2008; Lin and Gubb, 2009; Strutt et al., 2013). Similar dependence on a single Pk-Sple isoform is seen for A-abd, P-abd and eye (Gubb et al., 1999; Lawrence et al., 2004), and ectopic expression of the alternative isoform has been observed to produce reversals of polarity in A-abd and P-abd (Lawrence et al., 2004). These observations led to the proposal that the Pk and Sple isoforms have opposing effects on polarity, perhaps by differentially interpreting upstream directional information (Gubb et al., 1999; Lawrence et al., 2004).

To investigate this hypothesis, we performed a more rigorous test involving isoform 'swapping' in multiple tissues. As expected, we found that overexpressing Pk in a wing lacking both Pk and Sple (*pk-sple*) gives a hair and bristle pattern similar to that of wild type, whereas overexpressing Sple in a *pk-sple* wing reversed the direction of hair and bristle growth (Fig. 1C,D,E). Under similar conditions, Sple tagged with green fluorescent protein (GFP) localizes to the distal side of the cell, opposite to the proximal localization of Pk in wild-type wings (Strutt et al., 2013). This is indicative of reversal of the entire core complex, as confirmed here by the clonal expression of Vang::YFP (Fig. 2B,C). Similarly, swapping expression of the isoforms in A-abd and P-abd also reversed polarity (Fig. 1C′,D′,D″,E′,E″; see also Fig. 4). Thus, the direction of polarity is determined by the relative activities of Pk or Sple isoforms in wing, A-abd and P-abd.

### Pk-Sple isoforms differentially bias MT polarity in the wing

Because directional vesicular trafficking of the distal core protein Fz has been linked to the polarization of core proteins in the wild-type wing (Shimada et al., 2006), we determined the direction of Dsh

Development (2014) 141, 2866-2874 doi:10.1242/dev.105932

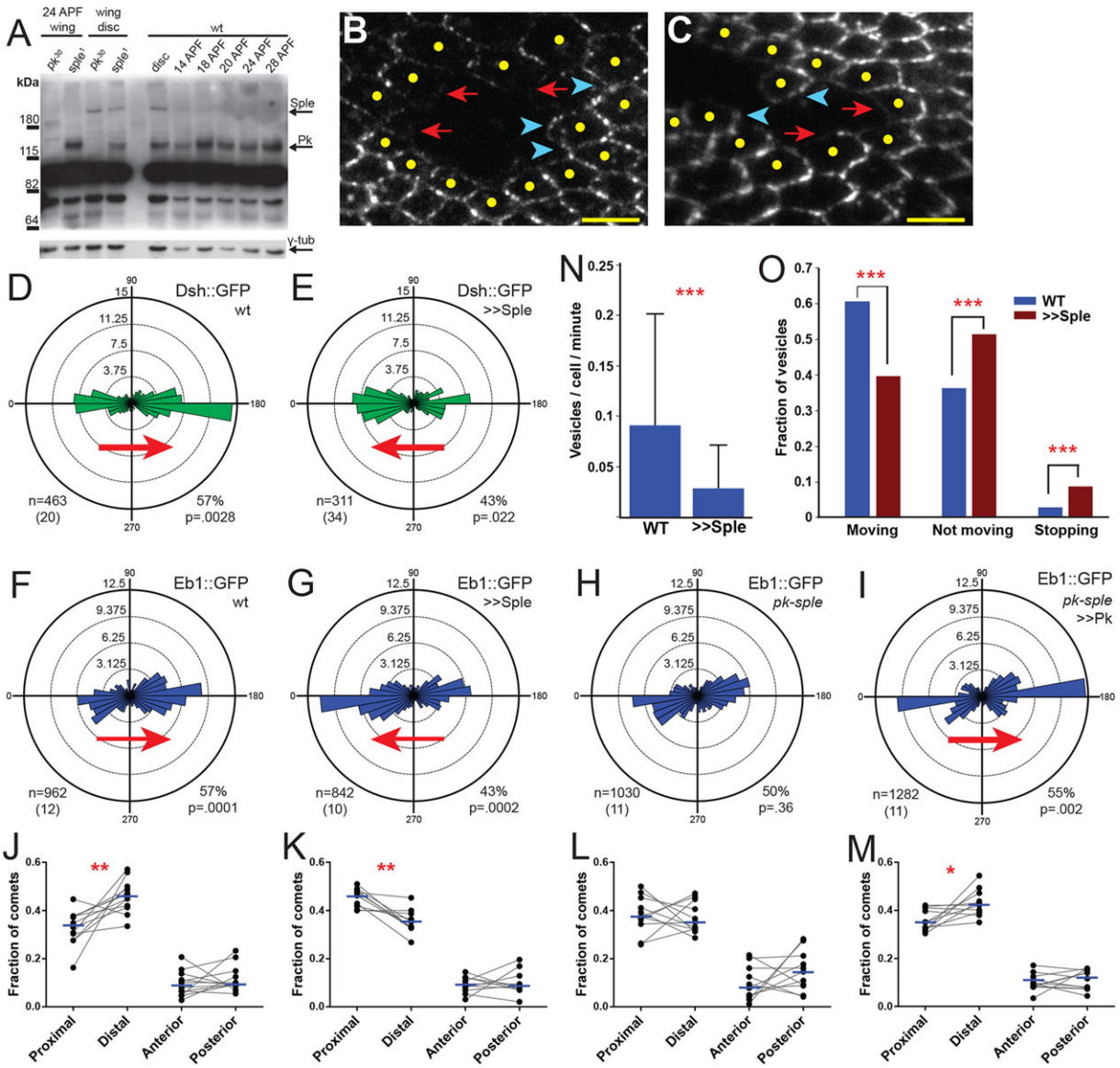


**Fig. 2. Effects of *pk* and *sple* isoform expression in wing.** (A) Western blot of Pk-Sple levels in the developing wing shows that Pk is the dominant isoform expressed in discs and pupal wings, whereas a very low level of Sple is detected in wing discs and early pupal wings. Note that the molecularly uncharacterized *sple*$^{1}$ allele reduces but does not eliminate expression. (B, C) Clonal analysis of Vang::YFP asymmetry in wild-type (wt, B) and Sple overexpressing (C) wings at 28 h APF. Yellow dots mark Vang::YFP expressing cells surrounding the clone. Blue arrowheads mark the sides of cells that are enriched for, and red arrows mark the sides depleted of, Vang::YFP. The proximal side is towards the left of the image. (D,E) Percentage of Dsh::GFP vesicles that moved in a given direction across the apical surface of cells in wild-type (D) and Sple overexpressing (>>Sple, E) wings from 22-24 h APF. (F-I) Percentage of Eb1::GFP comets that moved in a given direction across the apical surface of cells in wild-type (F), Sple overexpressing (G), *pk-sple* mutant (H) and *pk-sple, UAS-Pk* (>>Pk, I) wings at 24 h APF. For all circular plots: red arrows represent statistical significance for movement in the indicated direction; *n* is the total number of events (vesicles or comets); the number of flies is in parentheses; percentages indicate proportion of vesicles or comets moving towards the distal quadrant compared with the proximal quadrant of angles. (J-M) Fraction of Eb1::GFP comets in each fly that moved in a given direction in wild-type (J) (**$P$=0.0024), Sple overexpressing (K) (**$P$=0.0039), *pk-sple* (L) ($P$=0.83) and *pk-sple, UAS-Pk* (M) ($P$=0.014) wings; gray lines link values from the same fly; blue bars mark the median. (N) Comparison of the number of moving vesicles in wild-type ($n$=37 movies; 343 vesicles from 13 flies) and Sple overexpressing ($n$=98 movies; 298 vesicles from 30 flies) wings, ***$P$<0.001, mean±s.d. is shown. (O) Fraction of vesicles moving, not moving and transitioning from moving to stagnant (see Materials and Methods for definitions), measured 22-24 h APF in wild type ($n$=378 vesicles from 13 flies) and upon Sple overexpression ($n$=368 vesicles from 21 flies); ***$P$<0.001. See supplementary material Fig. S2B for schematic of where Dsh::GFP and Eb1::GFP measurements were made in the wing. Scale bars: 5 μm.

vesicular trafficking in the wing under conditions in which either the Pk or Sple isoform predominated. Consistent with previous results for Fz-containing vesicles (Shimada et al., 2006), we found that, in the Pk-predominant wild-type wing, Dsh-containing vesicles moved with an overall bias towards the distal sides of cells (Fig. 2D; supplementary material Movies 1 and 2) (M.M, unpublished). Many vesicles exited one membrane, traversed the cell and fused at an opposite membrane (for example, see supplementary material Movie 2). Furthermore, we used Eb1::GFP to visualize the growing plus-ends of MTs and confirmed that the Eb1::GFP 'comets', and hence the MTs on which the vesicles travel, have an overall distal plus-end bias, as reported previously (Shimada et al., 2006; Harumoto et al., 2010) (Fig. 2F,J; supplementary material Movie 3 and Fig. S2F,G). By contrast, in wings that overexpressed Sple, in

Development (2014) 141, 2866-2874 doi:10.1242/dev.105932

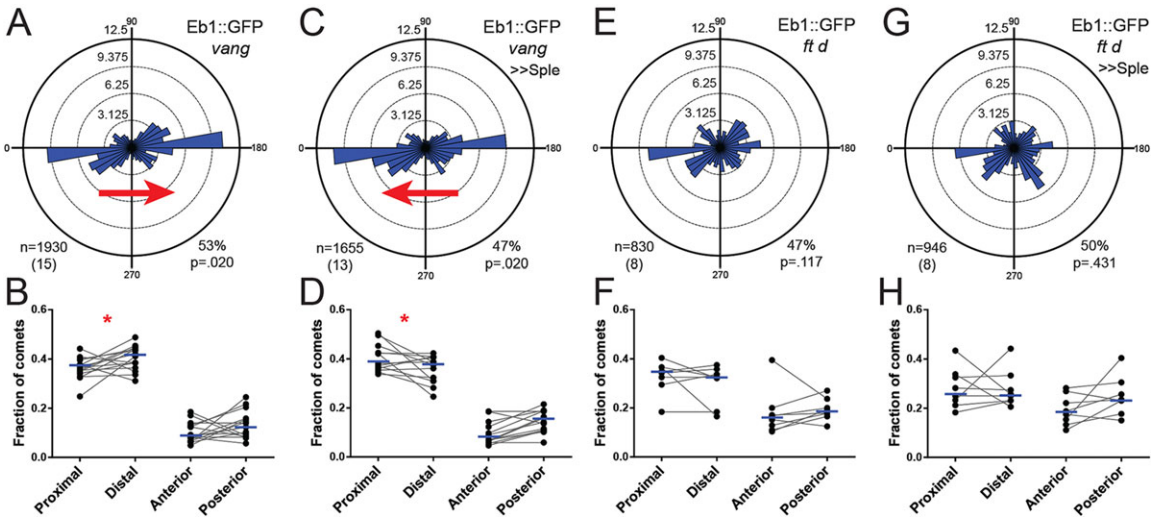


**Fig. 3. Dependence of Eb1 comet direction on *vang* and *ft*.** Fraction of Eb1::GFP comets moving in a given direction in the wing of *vang* mutant (A,B; **P*=0.0341); *vang, UAS-Sple* (C,D; **P*=0.0498); *ft-dachs* (E,F; *P*=0.5625); and *ft-dachs, UAS-Sple* (G,H; *P*=0.8438) flies. For detailed descriptions of circular plots and graphs, see Fig. 2 legend. >>Sple denotes overexpression of Sple.

which hairs and core proteins are reversed, Dsh::GFP vesicle movement was reversed, showing an overall bias towards the proximal sides of cells (Fig. 2E). Remarkably, we found that MT orientation was also reversed by Sple overexpression, as determined by the Eb1::GFP comet assay, producing a proximal plus-end bias (Fig. 2G,K). Thus, the direction of Dsh::GFP vesicle movement corresponds with the bias of MT plus-ends, which in turn depends on the expression of Pk or Sple, suggesting a mechanism by which Sple overexpression causes a reversal in the direction of hair growth and the localization of core proteins. The dependence of MT orientation on Pk-Sple is evident in third-instar wing discs, the stage at which MTs first emerge as dense bundles that appear in wild type as dots on the proximal side of the cell; however, these 'dots' were shifted towards the distal side upon overexpression of Sple (supplementary material Fig. S4).

These data indicate that, in the wing, Sple overexpression redirects MT orientation and, hence, transcytosis of Dsh. We find that the Pk isoform also directs the polarity bias of MTs: the observed Pk-dependent distal MT polarity bias in wild-type wings was lost in *pk-sple* mutant wings (Fig. 2H,L), yet overexpression of Pk rescued the wild-type distal plus-end polarity bias in these mutant wings (Fig. 2I,M).

### Control of MT polarity by Pk-Sple in the wing is independent of Vang but requres an intact Ft/Ds/Fj module

The ability to control MT orientation is specific to Pk-Sple because mutating *vang* or *fz* does not affect MT polarity bias (Harumoto et al., 2010). We confirmed that the plus-end distal bias was maintained in *vang* mutant flies and, furthermore, observed that in a *vang*-null wing, overexpression of the Sple isoform still reversed this bias (Fig. 3A-D). These observations suggest that this function of Pk-Sple to control MT orientation is distinct from any activity of the core module. In *vang* mutant wings, the plus-end bias is less pronounced with or without Sple overexpression when compared with wild-type wings. We speculate that this might be because Pk-Sple is partially dependent on Vang for membrane localization (Strutt et al., 2013).

In *ft* mutant wings (in which Hippo signaling has been rescued by the removal of *dachs*; Ambegaonkar et al., 2012), and in *ds* mutants (Harumoto et al., 2010), MTs were randomly oriented (Fig. 3E,F; supplementary material Fig. S5E), whereas in wild type, they were mainly parallel in the proximal-distal direction (Fig. 2F,J; supplementary material Fig. S5A). Furthermore, the parallel proximal-distal orientation of MTs was maintained in a *pk-sple* mutant wing (compare Fig. 3E,F and supplementary material Fig. S5E with Fig. 2H,L and supplementary material Fig. S5C). Therefore, parallel organization of the apical MT network depends on the Ft/Ds/Fj module, and the proximal-distal polarity bias depends upon Pk-Sple. Additionally, we found that Sple overexpression did not reorganize MT polarity in *ft dachs* double mutants (compare Fig. 3E,F with Fig. 3G,H). Therefore, the parallel organization of MTs is required in order to observe the polarizing activity of Sple and, by inference, Pk.

### Vesicle dynamics are altered in Sple overexpressing and *pk-sple* mutant wings

In Sple overexpressing wings that show reversed polarity of core PCP protein organization and hairs, Dsh::GFP vesicle movement was not only biased in the opposite direction, but those vesicles that moved did so more haltingly than in wild type (Fig. 2N,O). Furthermore, in Pk-predominant wild-type wings, we observed more Dsh::GFP vesicles than in *pk-sple* mutant wings, as has been reported previously for Fz::GFP vesicles (Harumoto et al., 2010); however, in Sple-overexpressing wings, the numbers of Dsh::GFP vesicles were similar to that of *pk-sple* wings, although it must be noted that the small numbers weakened the statistical power to detect differences. This is consistent with a core function for Pk in promoting vesicle trafficking, but not necessarily for Sple. However, our impression is that movement patterns are qualitatively different between *pk-sple* mutant wings and Sple overexpressing wings (compare Fig. 2E with supplementary material Fig. S2D). Thus, in addition to controlling the direction of MT polarity, Pk, but not necessarily Sple, promotes the vesicular transport of Dsh.

### Pk-Sple isoforms determine the direction of abdominal hair growth by biasing MT polarity

Biased MT-dependent vesicular trafficking of Fz and Dsh that is directed by Fj and Ds gradients is an attractive hypothesis for introducing asymmetry to the core module in all tissues. However, because the relative orientations of the Fj and Ds gradients with respect

Development (2014) 141, 2866-2874 doi:10.1242/dev.105932

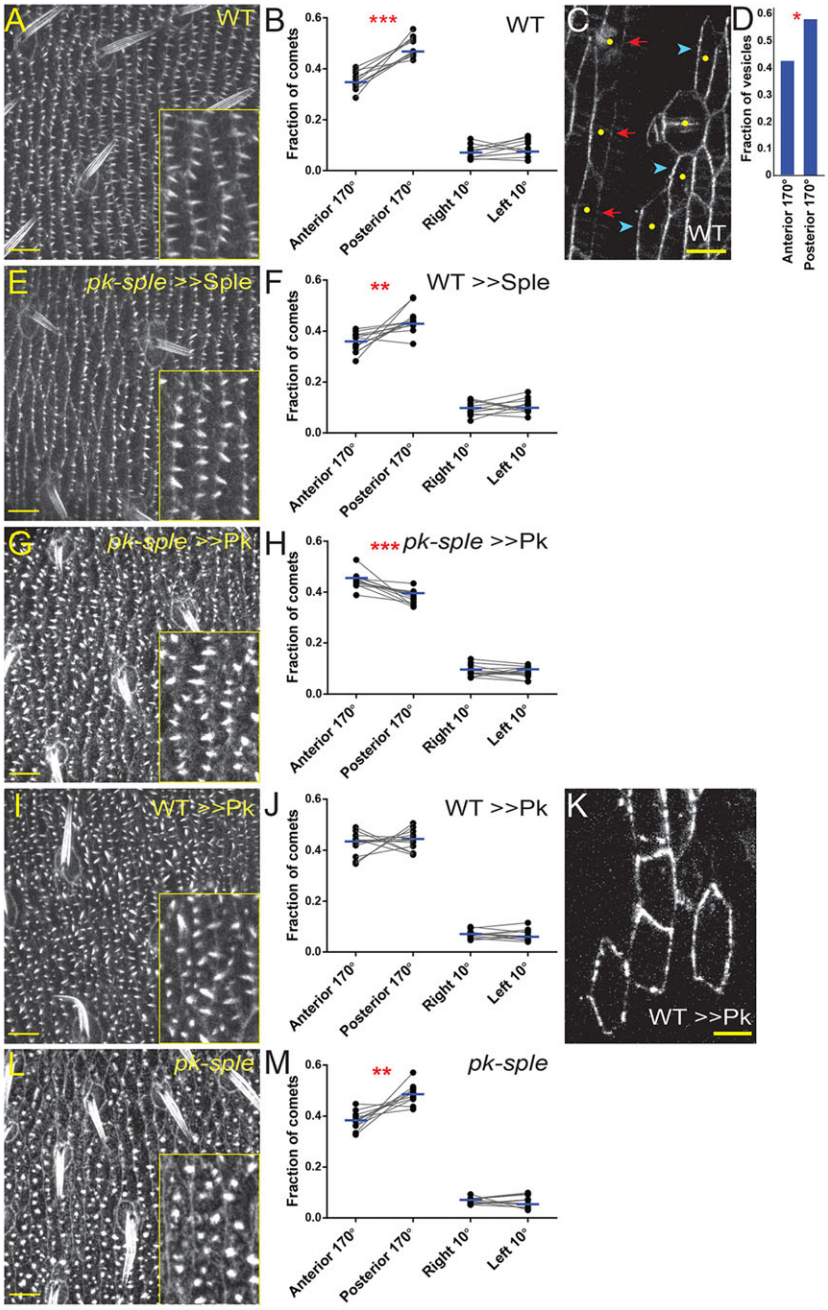


**Fig. 4. Effects of *pk* and *sple* isoform expression in A-abd.** (A,E,G,I,L) Phalloidin staining to visualize F-actin in pre-hairs of A-abd at 45 h APF. When *pk* expression is swapped for that of *sple*, the direction of hair growth is reversed. Insets show enlarged images of areas. (B,F,H,J,M) In each fly, the fraction of Eb1::GFP comets that moved in a given direction in (B) wild-type (WT; ***$P$=0.0010, 5282 comets from $n$=11 flies), (F) *UAS-Sple* (**$P$=0.0015, 3869 comets from $n$=12 flies), (H) *pk-sple, UAS-Pk* (***$P$=0.0005, 3895 comets from $n$=12 flies), (J) *UAS-Pk* ($P$=0.7334, 3642 comets from $n$=12 flies) and (M) *pk-sple* (**$P$=0.0020, 4004 comets from $n$=11 flies) A-abds. Gray lines link values from the same fly; blue bars mark the median. (C,K) Vang::YFP localized asymmetrically to the proximal side (blue arrowheads compared with distal red arrows) of cells in (C) wild-type but not (K) *pk* overexpressing A-abd. Yellow dots indicate center of Vang::YFP-expressing cells surrounding the clone. (D) Fraction of Dsh::GFP vesicles in wild-type A-abd that moved anteriorly or posteriorly ($n$=126 vesicles from 19 flies, *$P$=0.045). Anterior is to the left in all images. See supplementary material Fig. S2C for schematic of where, in A-abd phalloidin staining, Eb1::GFP comet and Dsh::GFP analyses were performed. >> denotes overexpression. Scale bars: 10 µm (A,E,G,I,L); 5 µm (C,K).

to the direction of core protein polarization are not conserved between tissues (Fig. 5A; Zeidler et al., 2000; Casal et al., 2002; Ma et al., 2003; Matakatsu and Blair, 2004; Rogulja et al., 2008; Axelrod, 2009), universality of this model requires that one explain how oppositely oriented gradient patterns can be rectified to produce similarly polarized outcomes. Our results provide a plausible answer to this rectification paradox. Tissues in which Fz and Dsh accumulate towards the low end of the Ds gradient (wing and P-abd) rely on the Pk but not the Sple isoform, whereas tissues in which Fz and Dsh accumulate away from the low end of the Ds gradient (eye and A-abd) rely on the Sple isoform (Gubb et al., 1999; Lawrence et al., 2004). We have shown that, in the wing, predominance of either the Pk or Sple isoform controls the direction of MT polarization, consistent with the model that the isoform predominance determines the direction of Ds and Fj gradient interpretation. One can hypothesize that a similar mechanism allows for rectification in other tissues, such as A-abd and P-abd, where one can infer that Sple and Pk are the predominant isoforms, respectively. Indeed, such a model has been suggested previously, except that no mechanism was proposed, and the upstream signal was thought not to be Ft/Ds/Fj (Lawrence et al., 2004, 2007; Lawrence and Casal, 2013).

To more broadly test the rectification function of alternative isoforms, we manipulated Pk and Sple expression in A-abd and P-abd, as we did in the wing, by removing both isoforms and replacing them with either Pk or Sple alone. As in the wing, and consistent with previous overexpression experiments (Lawrence et al., 2004; Lin and Gubb, 2009), we found that in both A-abd and P-abd, exchanging the isoforms reversed the polarity of hair growth (Fig. 1). This effect was more easily seen using phalloidin staining of pre-hairs (Fig. 4A,E,G). Pk caused hairs to point towards the low end of the Ds gradient, whereas Sple caused them to point towards the high end of the Ds gradient.

Development (2014) 141, 2866-2874 doi:10.1242/dev.105932

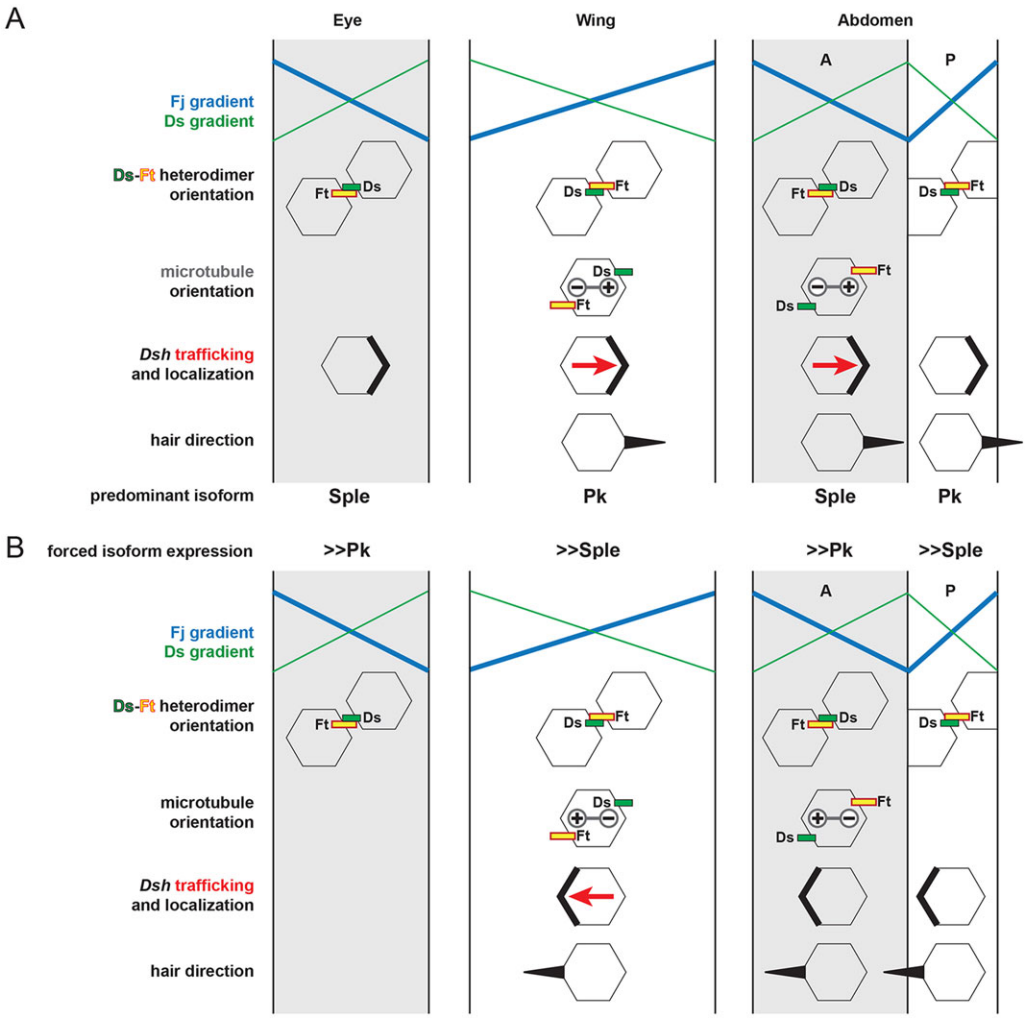


**Fig. 5. Organization of Ft/Ds/Fj and core PCP modules, and summary of previous and current results.** (A,B) The relative orientations of Fj and Ds gradients, the inferred or measured orientation of Ft/Ds heterodimers (Yang et al., 2002; Ma et al., 2003; Ambegaonkar et al., 2012; Bosveld et al., 2012; Brittle et al., 2012), the bias in MT orientation and the direction of Dsh vesicular trafficking and pre-hair initiation sites are shown for various tissue compartments in wild type (A) and upon forced expression (>>) of the alternative Pk and Sple isoforms (B). A, anterior; P, posterior.

To ask whether Pk-Sple isoform predominance regulates polarity in the abdomen by an MT-dependent mechanism similar to that in the wing, we first studied the wild-type A-abd, a Sple-predominant compartment, in more detail. In the A-abd compartment, pre-hairs arose from the posterior border of cells and pointed towards the posterior (Fig. 4A). MT plus-ends were also enriched towards the posterior (Fig. 4B; supplementary material Fig. S2H,I), showing the same relationship to the Fj and Ds gradients as those in wings that overexpressed Sple, and opposite to those in the wild-type wing (Fig. 2J,K). Correspondingly, Dsh::GFP vesicles moved posteriorly (Fig. 4D), and the expected organization of core PCP protein localization was observed, as assayed by the proximal localization of Vang::YFP (Fig. 4C). Therefore, consistent with the model proposed above, in this Sple-dependent compartment, MT polarity and Dsh vesicle direction exhibited the opposite relationship to the Fj and Ds gradients compared with the wild-type wing.

We then asked whether artificially controlling Pk and Sple expression regulates polarity in A-abd by polarizing MTs. When Sple was restored in a *pk-sple* background, normal polarity was restored (Fig. 4E); with forced expression of Sple, MTs were seen to point with plus-ends towards the posterior (Fig. 4F), as was seen in wild type. By contrast, when Pk was expressed in the *pk-sple* background, pre-hair polarity was almost perfectly reversed (Fig. 4G), and MT polarity was also reversed (Fig. 4H). However, when Pk was overexpressed in a wild-type background, where Sple is inferred to be predominant, we observed an intermediate phenotype, with some posterior pre-hairs but many arising from the center of the cell (Fig. 4I). In this condition, no MT plus-end polarity bias was detected (Fig. 4J), and little asymmetry of core PCP protein localization was observed using Vang::YFP as a marker (Fig. 4K). In pk-sple A-abd, polarity was severely disturbed, with many pre-hairs arising from the center of cells (Fig. 4L). Note that core PCP function is expected to be lost in the absence of either isoform. Surprisingly, in contrast to the wing, some residual posterior polarity of MTs was observed in the absence of either isoform (Fig. 4M). This polarity suggests that another source of Pk-Sple-independent information also polarizes these MTs in A-abd. In summary, these observations provide additional evidence that the predominance of the Pk and Sple isoforms determines the interpretation of the upstream directional signal in both wing and abdomen.

## DISCUSSION

Based upon our observations, and previous data summarized here, we propose a model for coupling Ft/Ds/Fj to the core module (Fig. 5A,B). Gradients of Fj and Ds, by promoting asymmetric distribution of Ft/Ds heterodimers, align a parallel network of apical MTs. Vesicles containing Dsh are transcytosed towards MT plus-ends. In the presence of Pk, MT plus-ends are biased towards the high end of the Fj gradient and the low end of the Ds gradient, whereas in the presence of Sple, the MT plus-ends are biased towards areas with low levels of Fj and high levels of Ds expression. Predominance of Pk or Sple,

Development (2014) 141, 2866-2874 doi:10.1242/dev.105932

therefore, determines how tissues differentially interpret, or rectify, the Ft/Ds/Fj signal to the core module. We hypothesize that this signal serves to both orient the breaking of initial symmetry and to provide continual directional bias throughout polarization. Additional validation of this model would require the measurement of Eb1::GFP comet directions while controlling Pk-Sple isoform expression in wings bearing ectopic Ds and Fj gradients, an experiment that is beyond our technical capabilities with currently available reagents. However, further evidence in support of this model is found in the observation that, in Pk-predominant wings, MT polarity and hair polarity point from regions with high toward low Ds expression both in wild-type wings and in wings with ectopic reversed Ds gradients (Harumoto et al., 2010).

We note that the distal plus-end bias of MTs is seen in much of the wild-type wing, but this bias decreases to equal proximal-distal plus-end distribution near to the most distal region of the wing (Harumoto et al., 2010) (and our unpublished observations). Thus, the mechanism described here might not affect the entirety of the wing; in contrast, plus-end bias was observed across the entire A-abd compartment (supplementary material Fig. S2C).

A model incorporating early Sple-dependent signaling and late Pk-dependent signaling has been proposed to explain PCP in the wing (Doyle et al., 2008; Hogan et al., 2011). Our observations and model are compatible with the data presented in support of that model; we saw that Sple expression, although always lower than Pk expression in wild-type wing, declined during pupal wing development, suggesting that, in *pk* mutants, polarity patterns might be set early in development, when Sple is still expressed (Fig. 2A) and when Ds is present in a stripe through the central part of the wing (Matakatsu and Blair, 2004; Rogulja et al., 2008; Hogan et al., 2011), giving rise to anteroposterior oriented patterns.

Pk (and presumably Sple, in Sple dependent compartments) is required for amplification of asymmetry by the core PCP mechanism (Tree et al., 2002; Amonlirdviman et al., 2005). Our results indicate an additional, core module independent, function for these proteins in regulating the polarity of MTs. Furthermore, although the core function of Pk-Sple is not well defined, part of that function might include promoting the formation and movement along aligned apical microtubules of Fz-, Dsh- and Fmi-containing vesicles (Shimada et al., 2006). The relative abundance of transcytosing vesicles in Pk versus Sple tissues suggests that if Sple promotes MT-dependent trafficking, it does so less efficiently than Pk.

These activities are remarkably similar to those that have been recently identified for Pk and Sple in fly axons, where Pk promotes or stabilizes MT minus-end orientation towards the cell body, and Sple promotes the orientation of minus-ends toward the synapse, which has effects on vesicle transport and neuronal activity (Ehaideb et al., 2014). We propose a common mechanism of differentially adapting the plus- and minus-ends of MT segments in both instances. In axons, similar to what we observe here, Pk also facilitates more robust cargo movement, whereas movement is less efficient when Sple is the dominantly expressed isoform (Ehaideb et al., 2014). Furthermore, MT polarity defects might underlie the apical-basal polarity defects and early lethality of mouse prickle1 mutant embryos (Tao et al., 2009). As Ft and Ds are not known to regulate MTs in axons, these observations suggest that Pk and Sple are able to modify MT polarity independently of Ft/Ds. However, in wings, a consequence is only evident if MTs are first aligned by Ft/Ds activity.

How Pk and Sple modulate the organization of MTs remains unknown, but possibilities include modifying the ability of Ft or Ds to capture or nucleate MTs, or altering plus-end dynamics to inhibit capture. These data also suggest the possibility of a more intimate link between the core PCP proteins and Ft/Ds than has been appreciated previously. We do not rule out other concurrent signals, such as that proposed for Wnt4 and Wg at the wing margin (Wu et al., 2013). However, the observations that (1) MTs correlate with the direction of core PCP polarization over space and time (Shimada et al., 2006; Harumoto et al., 2010), (2) vesicle transcytosis is disrupted in *ft* clones in which MTs are randomized (M.M., unpublished), (3) chemical disruption or stabilization of MTs disturbs polarity (Turner and Adler, 1998; Shimada et al., 2006) and (4) Pk and Sple isoform predominance rectifies signal interpretation by the core module in a fashion that follows both the wild-type and ectopic (Harumoto et al., 2010) Ds gradients provide additional evidence for the model that a signal from the Ft/Ds/Fj system orients the core PCP system in substantial regions of the wing and abdomen.

### Note added in proof

We refer the reader to related results in the following in-press report (Ayukawa et al., 2014). In addition to finding a function for the Pk-Sple isoform ratio in orienting the response to the Ft/Ds/Fj signal, the authors suggest a mechanism in which the unique N-terminal portion of Sple is coupled to Ds localization through interaction with Dachs. These results are consistent with our findings that Pk and Sple respond oppositely to Ft-Ds orientation and suggest an additional feature of the mechanism.

## MATERIALS AND METHODS

### Fly genotypes

The adult phenotypes were seen in flies of the following genotypes: (1) *OREGON-R*, (2) *D174Gal4;pk-sple$^{13}$/pk-sple$^{14}$; UAS-sple/+*, (3) *D174Gal4; pk-sple$^{13}$/pk-sple$^{14}$; UAS-pk::GFP/+* and (4) *D174Gal4; P{EP}pk[EP2557]/+*. For characterization of D174Gal4 see supplementary material Fig. S3. The genotypes used in Eb1 comet assays were: (5) *ciGal4/UAS-Eb1::GFP*, (6) *ciGal4, UAS-sple/UAS-Eb1::GFP*, (7) *pk-sple$^{13}$/pk-sple$^{14}$; ciGal4/UAS-Eb1::GFP*, (8) *pk-sple$^{14}$, UAS-pk/pk-sple$^{13}$; UAS-Eb1::GFP/ciGal4*, (9) *UAS-pk/+; ciGal4/UAS-Eb1::GFP*, (10) *vang$^{A3}$/vang$^{stbm6}$; ciGal4/UAS-Eb1::GFP*, (11) *vang$^{A3}$/vang$^{stbm6}$; ciGal4/UAS-Eb1::GFP, UAS-sple*, (12) *ft$^{8}$, d$^{1}$/ft$^{8}$, d$^{GC13}$; ciGal4/UAS-Eb1::GFP* and (13) *ft$^{8}$, d$^{1}$/ft$^{8}$, d$^{GC13}$; ciGal4/UAS-Eb1::GFP, UAS-sple*. The genotypes used in Vang asymmetry assays were: (14) *y w hsFLP; FRT42D Vang::YFP/FRT42D mRFP*, (15) *y w hsFLP; FRT42D Vang::YFP/FRT42D mRFP; ciGal4, UAS-sple/+* and (16) *y w hsFLP; actP-FRT-stop-FRT-Vang::YFP/UAS-pk; ciGal4/+*. The genotypes used for Dsh::GFP vesicle tracking were: (17) *Dsh::GFP (II)*, (18) *Dsh::GFP; hhGal4/UAS-mCherry*, (19) *Dsh::GFP; ciGal4, UAS-sple/+*, (20) *Dsh::GFP; ciGal4, UAS-sple, UAS-mCherry* and (21) *pk-sple$^{14}$, Dsh::GFP*. The genotype used in MT 'dot' assays in wing discs was: (22) *ciGal4/UAS-sple*. The genotypes used in MT immunostaining assays were: (1), (22), (23) *pk-sple$^{13}$/pk-sple$^{14}$*, (24) *UAS-pk/+; ciGal4/+* and (25) *ft$^{Gr\text{-}V}$ FRT40A/FRT40A Tub-Gal80; TubP-Gal4, UAS-mCD8::GFP/+*. The genotypes used in phalloidin staining assays were: (1), (23), (24), (26) *pk-sple$^{13}$/pk-sple$^{14}$; ciGal4/UAS-sple* and (27) *pk-sple$^{14}$, UAS-pk/pk-sple$^{13}$; ciGal4/+*.

### Western blot

Third-instar larval wing discs and pupal wings were dissected and lysed in protein loading buffer. Lysates from eight discs or wings were loaded per lane for SDS-PAGE analysis. Antibodies: (1) guinea pig antiserum was raised against a C-terminal fragment of Pk-Sple (amino acids 844-1116) that had been expressed as a 6×His fusion protein in *E. coli* and purified by using a Ni-NTA column (Qiagen) for injection (Josman); (2) mouse monoclonal antibody against γ-tubulin (Sigma-Aldrich).

### Live imaging of Eb1::GFP comet and Dsh::GFP vesicles

White pre-pupae were picked and aged in a humidified chamber at 25°C. Pupae were removed from their pupal cases (or a small window in the case

Development (2014) 141, 2866-2874 doi:10.1242/dev.105932

was opened) and mounted in Halocarbon oil 700 (Sigma-Aldrich). Movies were captured by using a Leica SP5 confocal microscope. The angles of Dsh::GFP vesicle and Eb1::GFP comet trajectories were tracked manually (comets with color-coded hyperstacks) using Fiji (Schindelin et al., 2012). Graphs were generated using GraphPad Prism6 (version 6 for Windows, GraphPad Software) and Oriana3 (Kovach Computing Services). In A-abd, Eb1::GFP comets were measured in the third dorsal segment (42 h APF), and Dsh::GFP vesicles were measured in dorsal segments 3-5 (41-47 h APF). Eb1 comets were included if they could be tracked for at least three frames (~15 s) and a clear track could be seen in the hyperstack for a given cell. Vesicles were grouped in three categories: (1) moving (vesicles that were observed to move and that were not categorized as stopping), (2) not moving (not observed to move at all) and (3) stopping (vesicles transitioning to a stagnant state without transitioning back to moving for more than 30 s).

### Statistical analysis of Eb1::GFP comets and Dsh::GFP vesicles

*P*-values for biases in comet and vesicle directions were calculated using a one-tailed binomial test where *n* was the number of comets or vesicles in all flies of a given genotype. The fraction of comets moving in a given direction was analyzed by using the Wilcoxon matched-pairs signed rank test where *n* was the number of flies of a given genotype. In the wing, the number of vesicles or comets moving distally (135° to 225°) and proximally (315° to 45°) were compared. In the abdomen, the number of vesicles or comets moving anteriorly (275° to 85°) and posteriorly (95° to 265°) were compared.

For comparing the fractions of vesicles that were moving, not moving or stopping, the fraction of vesicles observed in each category for wild type was used as the null hypothesis in one-tailed binomial tests to calculate the probability (*P*-values) for observed fractions with Sple overexpression.

The *P*-value for the difference in the total number of moving vesicles per cell per minute between wild type and Sple overexpression was calculated using the Wilcoxon rank sum test for equal medians.

### Clonal analysis of Vang::YFP asymmetry

Vials were heat-shocked at 37°C for 1 h to induce recombination. All tissue was wild type for endogenous *vang*. After 24-48 h, the pupae were picked, aged (28 h APF for wing, 47 h APF for A-abd) and mounted for live imaging, as described above.

### Analysis of MT 'dot' position

Sple was overexpressed in only the anterior compartment to directly compare wild-type and Sple overexpressing tissue. The localization of apical tubulin [antibody (YL1/2) ab6160 Abcam] in early third-instar larval wing pouches was analyzed using a cross correlation method, as described elsewhere (Matis et al., 2012), to measure the position of a tubulin 'dot' [relative to cell membrane, marked by using an antibody against Armadillo-c; N27A1 from the Developmental Studies Hybridoma Bank].

### Phenotypic analysis of adult tissue

Dissected tissue from female flies was mounted in Euparal (Asco Laboratories) that had been diluted with ethanol. *z*-stacks were captured by using a Spot Flex camera (Model 15.2 64 MP) coupled to a Nikon Eclipse E1000M microscope, the images were manually stacked using Adobe Photoshop and stitched in Fiji. The images shown are of dorsal wing and dorsal abdominal segments 3-5.

### Immunofluorescence and phalloidin staining

Dissected tissue from pupae at 24 h (wing) or 45 h (A-abd) APF was fixed in 4% paraformaldehyde with 0.1% Triton X-100. MTs in wing tissue were stained by using an antibody against α-tubulin (ab18251, Abcam). F-actin in abdominal pre-hairs was stained with Alexa Fluor 488-conjugated phalloidin (Molecular Probes).

#### Acknowledgements

We thank S. Collier, D. Tree and R. Holmgren for reagents; D. Tree for initial observations with EP2557; M. Simon for eye sectioning; and M. Simon and Axelrod laboratory members for critical readings of the manuscript.

#### Competing interests

The authors declare no competing financial interests.

#### Author contributions

J.D.A. conceived the study. J.O., K.A.S., B.C. and M.M. designed and performed all experiments and analyzed the data. All authors critically discussed and interpreted the data. J.D.A., K.A.S. and J.O. wrote, and all authors contributed to editing, the manuscript.

#### Funding

J.O. was supported by the Swedish Research Council; K.A.S. by a National Science Foundation Graduate Research Fellowship [1147470] and by NIH/NHGRI [5 T32 HG000044]; and M.M. by the AXA Research Fund. J.D.A. was supported by grants from the National Institutes of Health [GM059823 and GM097081]. Deposited in PMC for release after 12 months.

#### Supplementary material

Supplementary material available online at
http://dev.biologists.org/lookup/suppl/doi:10.1242/dev.105932/-/DC1

#### References

**Ambegaonkar, A. A., Pan, G., Mani, M., Feng, Y. and Irvine, K. D.** (2012). Propagation of Dachsous-Fat planar cell polarity. *Curr. Biol.* **22**, 1302-1308.

**Amonlirdviman, K., Khare, N. A., Tree, D. R., Chen, W.-S., Axelrod, J. D. and Tomlin, C. J.** (2005). Mathematical modeling of planar cell polarity to understand domineering nonautonomy. *Science* **307**, 423-426.

**Axelrod, J. D.** (2009). Progress and challenges in understanding planar cell polarity signaling. *Semin. Cell Dev. Biol.* **20**, 964-971.

**Ayukawa, T., Akiyama, M., Mummery-Widmer, J. L., Stoeger, T., Sasaki, J., Knoblich, J. A., Senoo, H., Sasaki, T. and Yamazaki, M.** (2014). Dachsous-dependent asymmetric localization of Spiny-legs determines planar cell polarity orientation in Drosophila. *Cell Rep.* (in press).

**Bosveld, F., Bonnet, I., Guirao, B., Tlili, S., Wang, Z., Petitalot, A., Marchand, R., Bardet, P.-L., Marcq, P., Graner, F. et al.** (2012). Mechanical control of morphogenesis by Fat/Dachsous/Four-jointed planar cell polarity pathway. *Science* **336**, 724-727.

**Brittle, A., Thomas, C. and Strutt, D.** (2012). Planar polarity specification through asymmetric subcellular localization of Fat and Dachsous. *Curr. Biol.* **22**, 907-914.

**Casal, J., Struhl, G. and Lawrence, P. A.** (2002). Developmental compartments and planar polarity in Drosophila. *Curr. Biol.* **12**, 1189-1198.

**Casal, J., Lawrence, P. A. and Struhl, G.** (2006). Two separate molecular systems, Dachsous/Fat and Starry night/Frizzled, act independently to confer planar cell polarity. *Development* **133**, 4561-4572.

**Chen, W.-S., Antic, D., Matis, M., Logan, C. Y., Povelones, M., Anderson, G. A., Nusse, R. and Axelrod, J. D.** (2008). Asymmetric homotypic interactions of the atypical cadherin flamingo mediate intercellular polarity signaling. *Cell* **133**, 1093-1105.

**Doyle, K., Hogan, J., Lester, M. and Collier, S.** (2008). The Frizzled Planar Cell Polarity signaling pathway controls Drosophila wing topography. *Dev. Biol.* **317**, 354-367.

**Eaton, S., Wepf, R. and Simons, K.** (1996). Roles for Rac1 and Cdc42 in planar polarization and hair outgrowth in the wing of *Drosophila*. *J. Cell Biol.* **135**, 1277-1289.

**Ehaideb, S., Iyengar, A., Ueda, A., Iocabucci, G., Cranston, K., Bassuk, A. G., Gubb, D., Axelrod, J. D., Gunawardena, S., Wu, C.-F. et al.** (2014). The seizure-associated gene prickle organizes microtubule polarity to modulate axonal transport. *Proc. Natl. Acad. Sci. USA* (in press).

**Fristrom, D. and Fristrom, J. W.** (1975). The mechanism of evagination of imaginal discs of Drosophila melanogaster: 1. General considerations. *Dev. Biol.* **43**, 1-23.

**Goodrich, L. V. and Strutt, D.** (2011). Principles of planar polarity in animal development. *Development* **138**, 1877-1892.

**Gubb, D., Green, C., Huen, D., Coulson, D., Johnson, G., Tree, D., Collier, S. and Roote, J.** (1999). The balance between isoforms of the prickle LIM domain protein is critical for planar polarity in Drosophila imaginal discs. *Genes Dev.* **13**, 2315-2327.

**Harumoto, T., Ito, M., Shimada, Y., Kobayashi, T. J., Ueda, H. R., Lu, B. and Uemura, T.** (2010). Atypical cadherins dachsous and fat control dynamics of noncentrosomal microtubules in planar cell polarity. *Dev. Cell* **19**, 389-401.

**Hogan, J., Valentine, M., Cox, C., Doyle, K. and Collier, S.** (2011). Two frizzled planar cell polarity signals in the Drosophila wing are differentially organized by the Fat/Dachsous pathway. *PLoS Genet.* **7**, e1001305.

**Lawrence, P. A. and Casal, J.** (2013). The mechanisms of planar cell polarity, growth and the Hippo pathway: some known unknowns. *Dev. Biol.* **377**, 1-8.

**Lawrence, P. A., Casal, J. and Struhl, G.** (2004). Cell interactions and planar polarity in the abdominal epidermis of Drosophila. *Development* **131**, 4651-4664.

**Lawrence, P. A., Struhl, G. and Casal, J.** (2007). Planar cell polarity: one or two pathways? *Nat. Rev. Genet.* **8**, 555-563.

Development (2014) 141, 2866-2874 doi:10.1242/dev.105932

**Lee, H. and Adler, P. N.** (2002). The function of the frizzled pathway in the Drosophila wing is dependent on inturned and fuzzy. *Genetics* **160**, 1535-1547.

**Lin, Y.-Y. and Gubb, D.** (2009). Molecular dissection of Drosophila Prickle isoforms distinguishes their essential and overlapping roles in planar cell polarity. *Dev. Biol.* **325**, 386-399.

**Ma, D., Yang, C.-H., McNeill, H., Simon, M. A. and Axelrod, J. D.** (2003). Fidelity in planar cell polarity signalling. *Nature* **421**, 543-547.

**Matakatsu, H. and Blair, S. S.** (2004). Interactions between Fat and Dachsous and the regulation of planar cell polarity in the Drosophila wing. *Development* **131**, 3785-3794.

**Matis, M., Axelrod, J. D. and Galic, M.** (2012). A universal analysis tool for the detection of asymmetric signal distribution in microscopic images. *Dev. Dyn.* **241**, 1301-1309.

**Müsch, A.** (2004). Microtubule organization and function in epithelial cells. *Traffic* **5**, 1-9.

**Rogulja, D., Rauskolb, C. and Irvine, K. D.** (2008). Morphogen control of wing growth through the Fat signaling pathway. *Dev. Cell* **15**, 309-321.

**Schindelin, J., Arganda-Carreras, I., Frise, E., Kaynig, V., Longair, M., Pietzsch, T., Preibisch, S., Rueden, C., Saalfeld, S., Schmid, B. et al.** (2012). Fiji: an open-source platform for biological-image analysis. *Nat. Methods* **9**, 676-682.

**Shimada, Y., Yonemura, S., Ohkura, H., Strutt, D. and Uemura, T.** (2006). Polarized transport of frizzled along the planar microtubule arrays in Drosophila wing epithelium. *Dev. Cell* **10**, 209-222.

**Strutt, D. and Strutt, H.** (2007). Differential activities of the core planar polarity proteins during Drosophila wing patterning. *Dev. Biol.* **302**, 181-194.

**Strutt, H. and Strutt, D.** (2008). Differential stability of flamingo protein complexes underlies the establishment of planar polarity. *Curr. Biol.* **18**, 1555-1564.

**Strutt, H. and Strutt, D.** (2009). Asymmetric localisation of planar polarity proteins: mechanisms and consequences. *Semin. Cell Dev. Biol.* **20**, 957-963.

**Strutt, H., Thomas-MacArthur, V. and Strutt, D.** (2013). Strabismus promotes recruitment and degradation of farnesylated prickle in Drosophila melanogaster planar polarity specification. *PLoS Genet.* **9**, e1003654.

**Tao, H., Suzuki, M., Kiyonari, H., Abe, T., Sasaoka, T. and Ueno, N.** (2009). Mouse prickle1, the homolog of a PCP gene, is essential for epiblast apical-basal polarity. *Proc. Natl. Acad. Sci. U.S.A.* **106**, 14426-14431.

**Tree, D. R. P., Shulman, J. M., Rousset, R., Scott, M. P., Gubb, D. and Axelrod, J. D.** (2002). Prickle mediates feedback amplification to generate asymmetric planar cell polarity signaling. *Cell* **109**, 371-381.

**Turner, C. M. and Adler, P. N.** (1998). Distinct roles for the actin and microtubule cytoskeletons in the morphogenesis of epidermal hairs during wing development in Drosophila. *Mech. Dev.* **70**, 181-192.

**Wu, J. and Mlodzik, M.** (2008). The frizzled extracellular domain is a ligand for Van Gogh/Stbm during nonautonomous planar cell polarity signaling. *Dev. Cell* **15**, 462-469.

**Wu, J., Roman, A.-C., Carvajal-Gonzalez, J. M. and Mlodzik, M.** (2013). Wg and Wnt4 provide long-range directional input to planar cell polarity orientation in Drosophila. *Nat. Cell Biol.* **15**, 1045-1055.

**Yang, C.-H., Axelrod, J. D. and Simon, M. A.** (2002). Regulation of Frizzled by fat-like cadherins during planar polarity signaling in the Drosophila compound eye. *Cell* **108**, 675-688.

**Zeidler, M. P., Perrimon, N. and Strutt, D. I.** (2000). Multiple roles for four-jointed in planar polarity and limb patterning. *Dev. Biol.* **228**, 181-196.

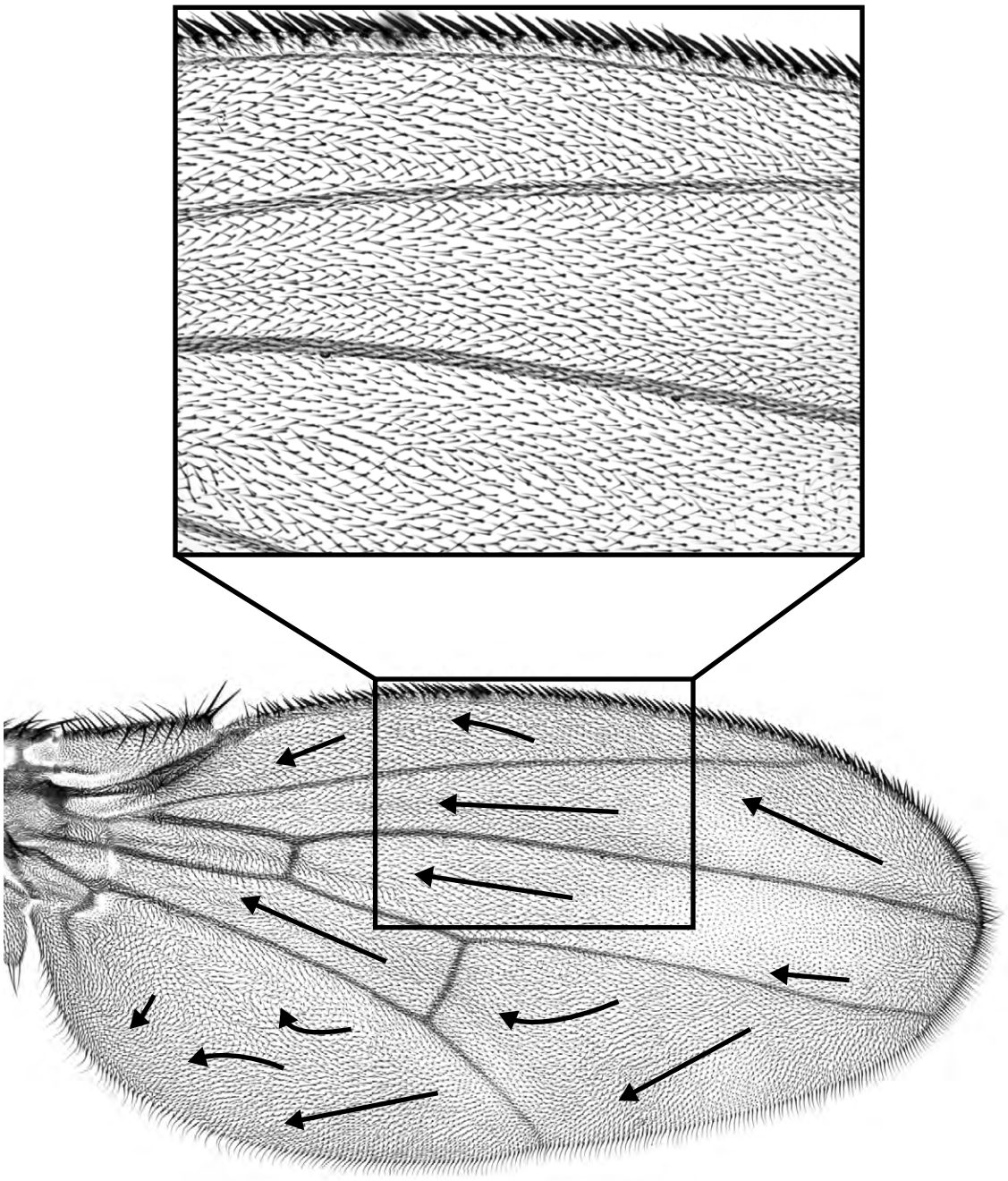

**Fig. S1. Overexpressing Sple in wing reverses hair polarity.** Wing overexpressing Sple using *D174Gal4* (see Fig. S3 for *D174Gal4* expression pattern) to drive expression of P{EP}pk[EP2557], inserted in the *pk* locus upstream of the *sple* start site. Note that hairs are more parallel using this overexpression method as compared to *D174Gal4, UAS-sple* (Fig. 1D), likely due to differences in levels or uniformity of expression.

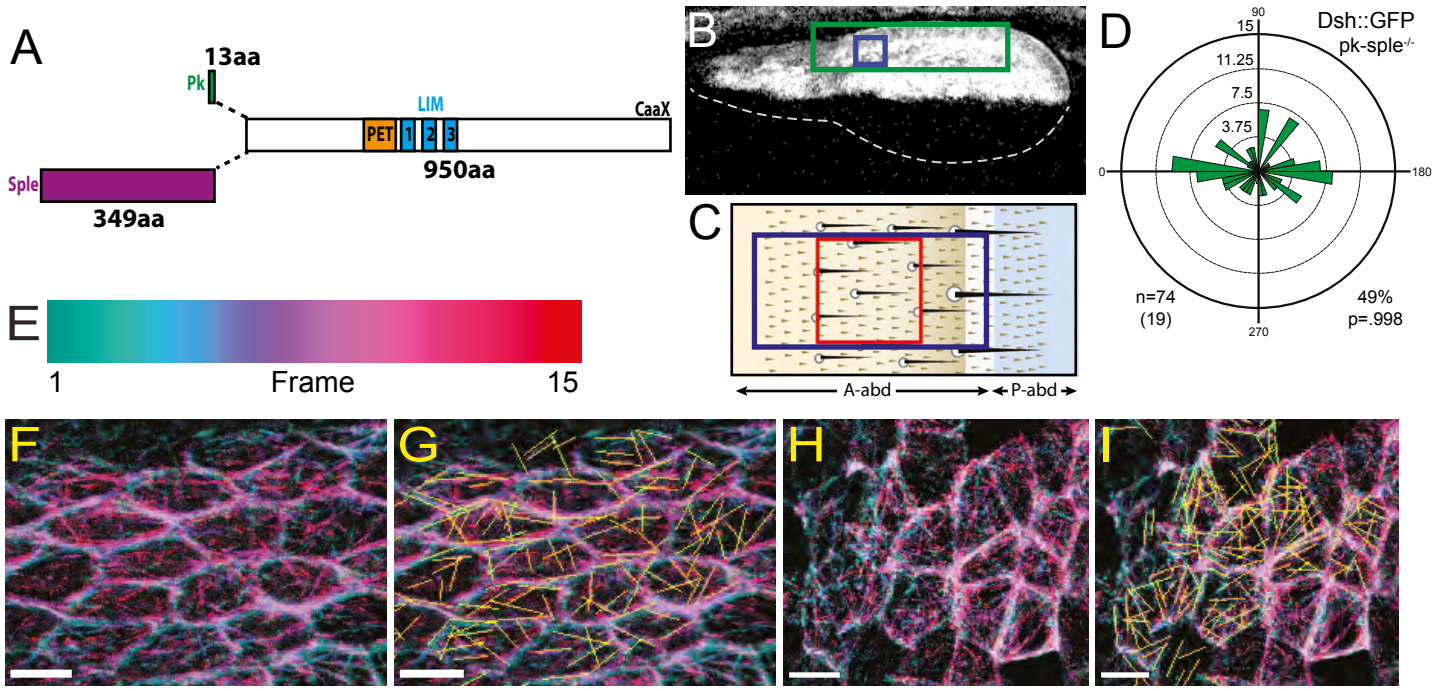


**Fig. S2.** **(A)** Schematic of Pk and Sple protein isoforms. The common portion contains one PET and three LIM domains in addition to a C-terminal CaaX membrane localization motif (Lin and Gubb, 2009). **(B)** Pupal wing expressing Eb1::GFP in the anterior compartment. Dotted line outlines the rest of the wing. Blue and green boxes indicate where Eb1::GFP comets and Dsh::GFP vesicles were measured, respectively. **(C)** Schematic of one abdominal segment. Blue box denotes where Eb1::GFP and Dsh::GFP measurements were made. Red box denotes location of Phalloidin-stained images. **(D)** Percentage of Dsh::GFP vesicles that moved in a given direction across the apical surface of cells in *pk-sple* wings, measured 22-25 h APF. **(E to I)** Color coded hyperstacks were used to analyze Eb1::GFP comets. These hyperstacks are maximum projections over time in which each frame is coded a different color on a scale from green to red (E): wt wing (F) with yellow overlays of traced comets (G) and wt A-abd (H,I). Scale bar=5 microns.

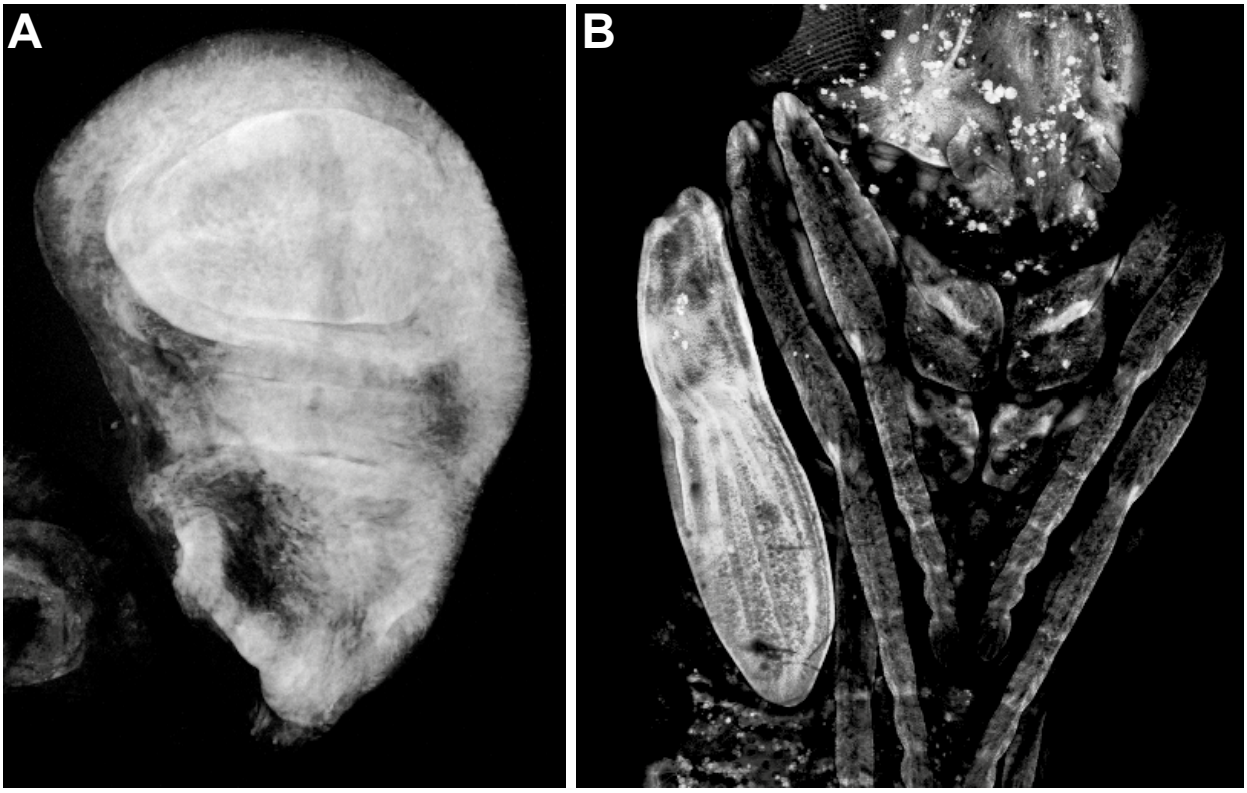


**Fig. S3. D174Gal4 expression**. D174Gal4 driving UAS-Eb1::GFP expression in a 3rd instar larval wing disc (A) and a 24 hour APF pupa (B).

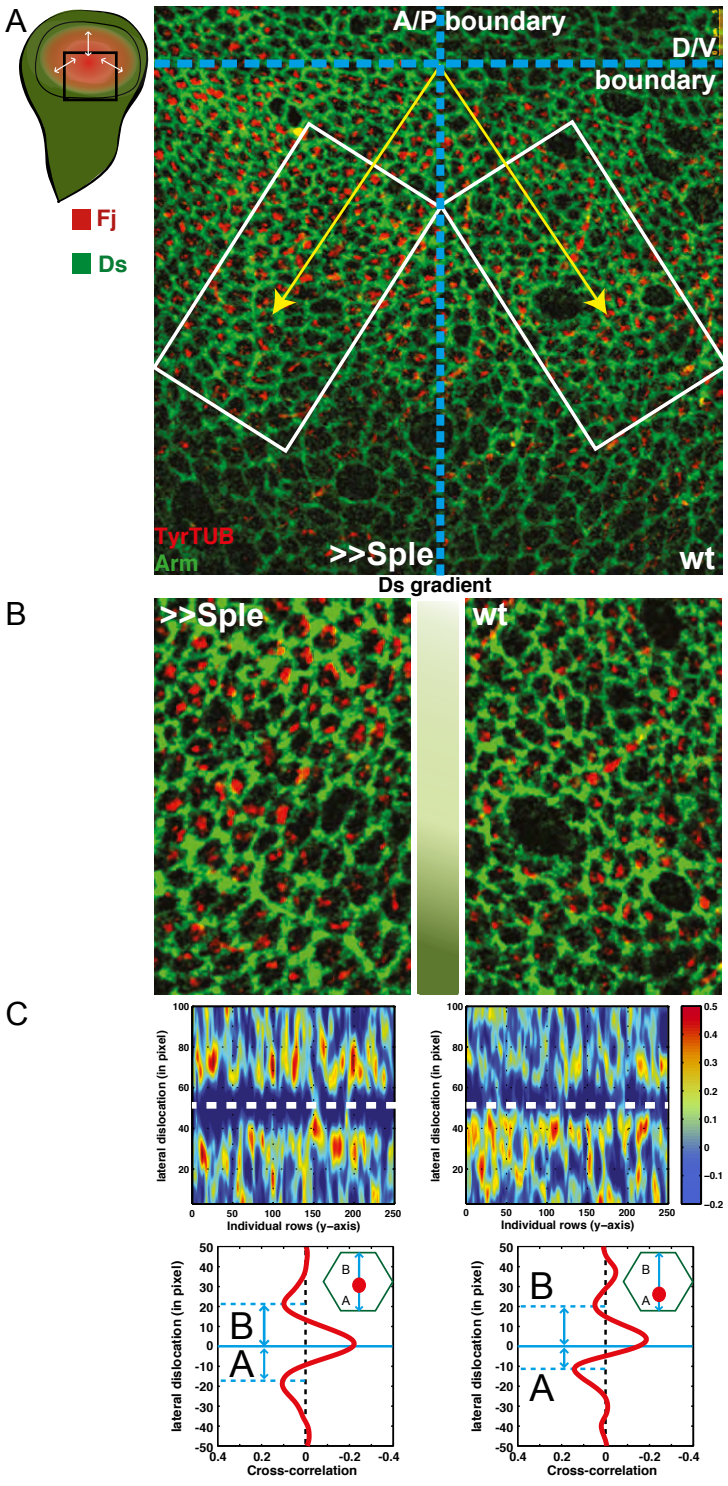


**Fig. S4. Site of initial MT accumulation in third instar wing discs depends on Pk and Sple. (A)** Third instar discs overexpressing Sple in the anterior compartment, and stained for Tyrosinated tubulin (TyrTUB; red) and Armadillo (Arm; green). **(B)** Regions demarcated by white boxes in (A), oriented according to the Ds gradient (green strip), showing that Tubulin dots tend to localize on the side of the cell toward the high end of the Ds gradient (proximal in wing disc) in the wt half, but are shifted toward the distal side of the cell in the Sple overexpressing half of the disc. Note that some cells show a strong shift, while others not at all, likely due to non-uniform expression of Sple. **(C)** The cross-correlation method (Matis et al., 2012) was used to quantify asymmetry. Similar results were obtained for analyses of four discs (a representative example is shown).

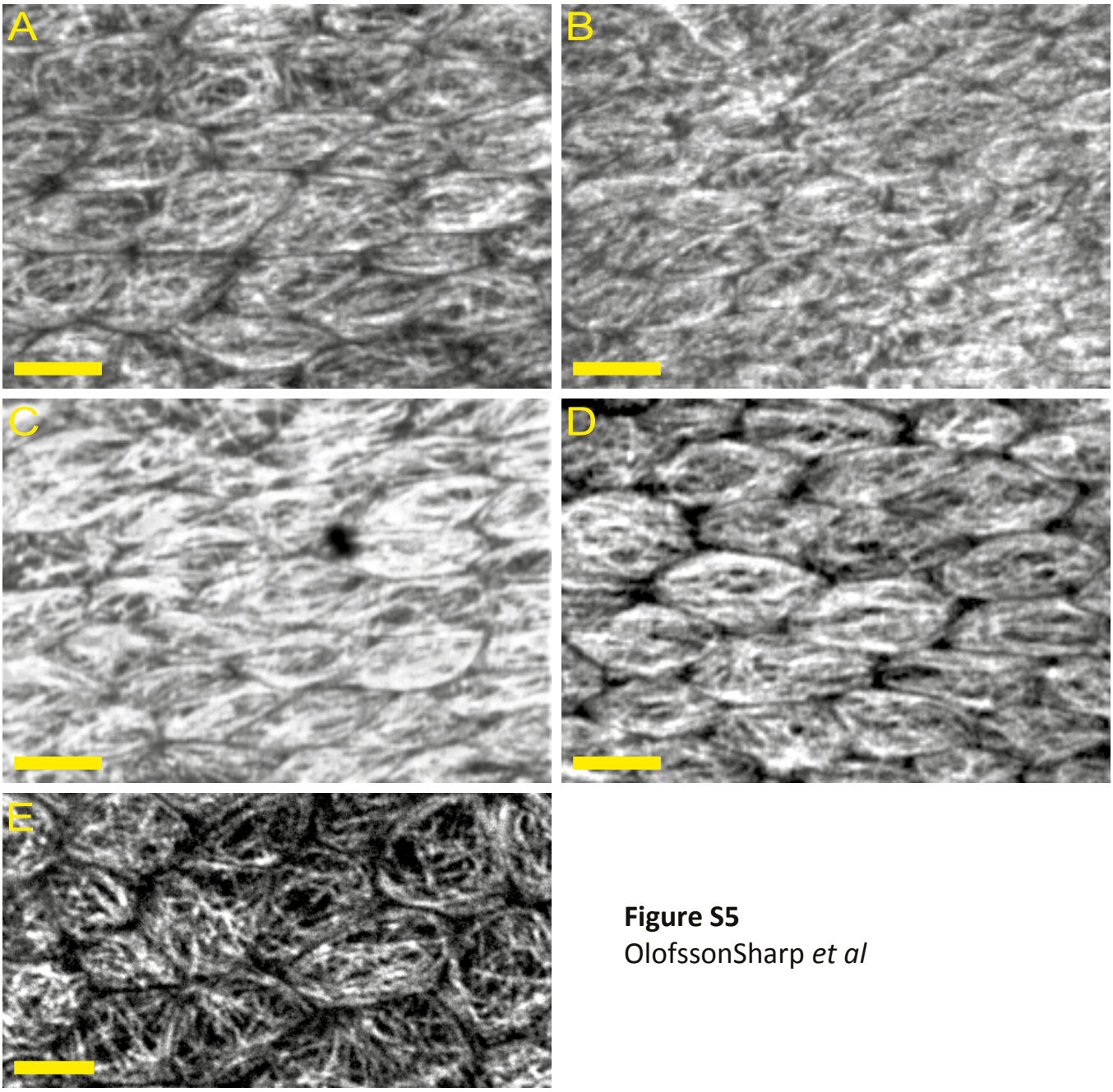


**Figure S5**
OlofssonSharp *et al*

**Fig. S5. Apical MT network orientation.** MT's are aligned parallel to the proximal-distal axis in wt **(A)**, Sple overexpressing **(B)**, *pk-sple* **(C)**, and Pk overexpressing **(D)** wings. In *ft* tissue, MT's are randomly oriented **(E)**. In all images, proximal is to the left, scale bar= 5 microns.

**Supplementary Movies:**

Original movies were 1 frame every 5.25 seconds. Playback rate increased here for viewability.


**Movie S1.** Cells in a wt wing exhibiting a range of described types of Dsh::GFP vesicle movement.


**Movie S2.** In wt wing, a Dsh::GFP vesicle is observed to traverse the entire length of the apical surface.


**Movie S3.** EB1::GFP comets moving on the apical surface of cells in a wt wing.